Cement & Concrete Composites 32 (2010) 116–120

Contents lists available at ScienceDirect

Cement & Concrete Composites

journal homepage: www.elsevier.com/locate/cemconcomp

Influence of cement type on ITZ porosity and chloride resistance of self-compacting concrete

Andreas Leemann *, Roman Loser, Beat Münch

Empa, Swiss Federal Laboratories for Materials Testing and Research, Überlandstr. 129, CH-8600 Dübendorf, Switzerland

ARTICLE INFO

Article history:
Received 1 October 2008
Received in revised form 10 November 2009
Accepted 13 November 2009
Available online 20 November 2009

Keywords:
Interfacial transition zone
Permeability
Blended cement
Self-compacting concrete

ABSTRACT

With the increasing use of self-compacting concrete (SCC) its durability has come into focus. Concerning the microstructure of concrete, the porosity in the interfacial transition zone (ITZ) is regarded as a key feature for permeability and durability. Generally, a combination of cement and mineral admixtures is used for the production of SCC. In the present study, ITZ porosity of four SCC mixtures produced with ordinary Portland cement, Portland limestone cement, slag cement and ordinary Portland cement combined with fly ash is analyzed. Additionally, the chloride migration coefficient is determined. ITZ porosity and width of the SCC mixtures are similar. The substantial differences in the chloride migration coefficients show that the binder type has a stronger influence on permeability than the pore volume in the ITZ.

1. Introduction

The porosity in the interfacial transition zone (ITZ) is recognized as a key feature with regard to the properties of mortar and concrete as it is larger than the porosity of the bulk paste [1–5]. Apart from the "wall effect" caused by poor particle packing leading to a locally increased water content, there are additional parameters affecting ITZ porosity such as water-to-binder ratio (w/b) of the concrete, binder composition or duration of mixing [6–8]. With the worldwide increasing use of self-compacting concrete (SCC), the question of its durability is of interest [9]. On the macroscopic scale, the durability of structures is improved because SCC potentially leads to more homogeneous concrete properties due to the lack of vibration induced segregation [10,11]. On the microscopic scale, the absence of vibration reduces the volume of water accumulating around aggregates and leads to lower ITZ porosity and lower permeability [12]. In the production of SCC, cement is often partly substituted by mineral admixtures in order to decrease heat of hydration and material cost or to improve flow properties [13–16]. So far, no quantitative data exist about the influence of different mineral admixtures or cement types on ITZ porosity of SCC. This topic is of increasing importance for conventionally vibrated concrete (CVC) as well, as more mineral admixtures and blended cements are used due to the problems related with CO_2 emission in cement production.

In this project, a possible connection between binder, ITZ porosity, bleeding and permeability is investigated. ITZ porosity of SCC mixtures produced with four different binders is analysed. The macroscopic properties of the concrete are characterized by determining compressive strength and chloride migration coefficients. Additionally, the bleeding of self-compacting mortars produced with the same binders as the SCC mixtures is measured.

2. Materials and methods

2.1. Materials and mix design

Table 1 shows the mix designs of the SCC mixtures and their workability. The self-compacting mortars (SCM) contain the same components as the concrete while omitting the gravel and reducing the w/b by 0.03. Four different binders were used for mortar and concrete (Tables 1–3): ordinary Portland cement (OPC, CEM I 42.5 N), Portland limestone cement (CEM II/A-LL 42.5 N), Portland slag cement (CEM III/A) and ordinary Portland cement in combination with low CaO fly ash (CEM I 42.5 N + V). The grain size distribution of the binders is shown in Fig. 1. Natural sand and gravel with a grain size distribution of 0–16 mm were used as aggregates (Fig. 2). The added superplasticizer was based on polycarboxylate ether.

SCC prisms with a size of 120 × 120 × 360 mm were produced and stored at 20 °C and 90% relative humidity for 24 h. After demolding they were put in saturated calcium hydroxide solution for 62 days. The long curing period was chosen because of the relatively slow hydration of fly ash and slag.

* Corresponding author. Tel.: +41 44 823 44 89; fax: +41 44 823 40 35.
E-mail address: andreas.leemann@empa.ch (A. Leemann).

0958-9465/$ - see front matter © 2009 Elsevier Ltd. All rights reserved.
doi:10.1016/j.cemconcomp.2009.11.007

Table 1
Composition and workability of the SCC mixtures.

Concrete	SCC I	SCC II	SCC III	SCC FA
Aggregates 0–16 mm (kg/m^3)	1735	1735	1735	1734
Sand/gravel-ratio	1	1	1	1
CEM I 42.5 N (kg/m^3)	455	–	–	353
CEM II/A-LL 42.5 N (kg/m^3)	–	451	–	–
CEM III/A 32.5 R (kg/m^3)	–	–	446	-
Low CaO fly ash (kg/m^3)	–	–	–	88
Superplasticizer (kg/m^3)	7.28	6.32	4.46	6.18
Water (kg/m^3)	178	177	175	173
Water-to-binder-ratio	0.4	0.4	0.4	0.4
Volume of paste (l/m^3)	330	330	330	331
Flow (cm)	62	64	68	64
Flow time L-box (s)	4.2	2.2	3.4	3.4

Table 2
Types of binders.

Type of binder according to EN 197-1	Abbreviation	Density (g/cm^3)	Blaine (cm^2/g)	Median (μm)
CEM I 42.5 N	CEM I	3.13	2970	19.6
CEM II/A-LL 42.5 N	CEM II	3.07	4320	17.5
CEM III/A 32.5 N	CEM III	2.99	4134	14.4
Fly ash	FA	2.13	2370	40.8

Table 3
Composition of binders.

Binder	CaO	SiO_2	Al_2O_3	Fe_2O_3	MgO	K_2O	Na_2O	SO_3
CEM I	63.8	19.8	4.7	2.7	1.9	1.02	0.18	3.1
CEM II	62.4	17.7	4.2	2.5	1.7	0.91	0.12	3.1
CEM III	50.8	27.3	7.1	1.7	4.0	1.00	0.13	2.8
FA	1.9	56.0	25.0	8.7	3.1	3.3	0.2	0.0

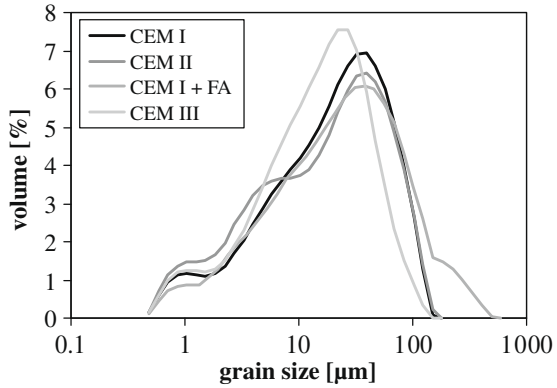

Fig. 1. Grain size distribution of the binders.

2.2. Methods for analysis

After production, the SCM mixtures were filled in upright prism formworks with dimensions of 40 × 40 × 160 mm and their top was covered with a sealed glass plate. Three prisms were produced per mixture. The water accumulating at the top was collected at the time of 15, 30, 60, 120 and 240 min after production. The experiment was conducted at 20 °C and 90% relative humidity.

Compressive strength of SCC was measured on the prisms at a sample age of 63 days according to [17]. The chloride resistance was determined on five cores (diameter and height of 50 mm)

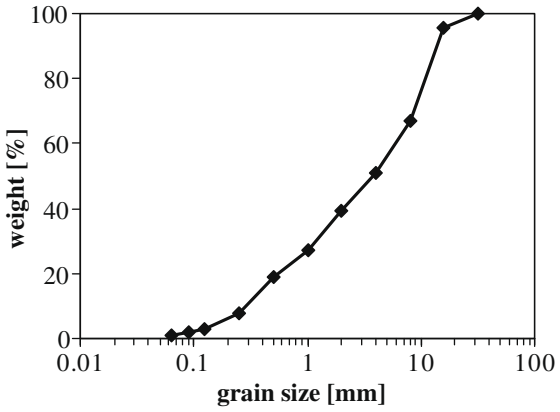

Fig. 2. Grain size distribution of the aggregates.

per mixture. In the rapid chloride migration test according to Swiss standard SIA 262/1 [18], chloride ingress in the water saturated samples is accelerated by applying a voltage of 20 mV during 24 h. From the depth of chloride ingress, a chloride migration coefficient D_m (non-steady state) was calculated.

In order to analyse the microstructure, cores with a diameter of 50 mm were taken in vertical direction, cut along the length axis, dried at 50 °C for three days, impregnated with epoxy resin containing a fluorescent dye and polished. Aggregates with a diameter >4 mm were randomly selected and examined with an optical microscope in order to assess the angle of intersection between aggregate surface and polished plane as described in [12]. Only aggregates which were cut more or less equatorially were selected for analysis in order to avoid an overestimation of ITZ thickness. Afterwards, the samples were coated with carbon and studied with a Philips ESEM-FEG XL30. The operating conditions of the ESEM were 15 kV in the high vacuum mode using a back-scatter detector. Ten aggregates were analysed per concrete mixture. Three images at the top of each aggregate, three at the side and three at the bottom were taken resulting in 90 images per SCC mixture (e.g. Fig. 3). The pictures had a resolution of 1420 × 968 pixels (pixel size: 0.22 × 0.24 μm) and a base length of 315 μm. A software for segmentation of the phases and subsequent evaluation of their distribution as a function of the distance to the aggregate has been developed in Matlab. The pictures were segmented to three different classes based on their grey scale values: main aggregates, pores and background (cracks and air voids). Due to the magnification used, the resolution was not sufficient to resolve capillary pores. Hence, the segmented "pores" represent porous zones. In SCC I, portlandite ($Ca(OH)_2$) and anhydrous cement were analysed in

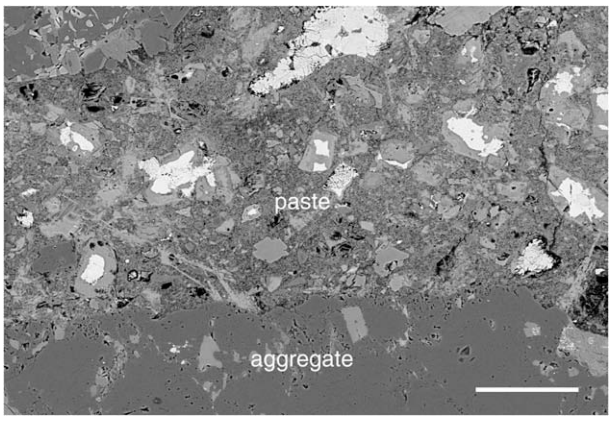

Fig. 3. SEM image in backscattering mode of the top of the aggregate in SCC I. The white bar has a length of 50 μm.

addition to the pores. In SCC III, an analysis of anhydrous cement including slag was added. In order to compare ITZ thickness of the different SCC mixtures, the boundary separating bulk paste and ITZ had to be defined. Paste in a distance of the aggregate >70 μm was defined as "bulk paste" and its average porosity was calculated. The ITZ was defined as the zone close to the aggregates where the current porosity exceeds the average of the bulk paste by 15%.

3. Results

3.1. Bleeding

The SCM mixtures show the highest bleeding rate within the first hour after production (Fig. 4). The differences between the different SCM are relatively small with SCM I showing the highest and SCM FA the lowest amount of bleeding water.

3.2. Macroscopic properties

The different SCC mixtures show a similar compressive strength (Fig. 5). However, chloride migration coefficients are significantly different. In order to show a typical relationship between chloride migration coefficient and compressive strength, values of three conventionally vibrated concrete mixtures (CVC FA: *w/c* of 0.35, 0.45 and 0.60) produced with the same binder as SCC FA have been added to Fig. 5 (published in [19]).

3.3. Microstructure

Pores are distributed inhomogeneously in the ITZ. As an example, pore distribution of SCC I (at the top of the aggregates) is shown in Fig. 6. The standard deviation gives an impression of the variation among the 30 different images (from 10 aggregates) analyzed. Average ITZ thickness of the various SCC mixtures is not substantially different (Fig. 7). The porosity increase towards the aggregates is interrupted in a distance between 5 and 20 μm in case of SCC I, SCC II and SCC FA. It is only slightly increasing in this area and forms a kind of plateau. However, porosity of SCC III is increasing continuously. The highest pore volume of all SCC mixtures is reached directly at the boundary to the aggregate. All SCC mixtures show a difference in ITZ porosity at the top, the side and the bottom of the aggregates (Fig. 8). The lowest porosity and the smallest ITZ thickness always occur at the top of the aggregates. The difference between top and side/bottom is substantial, while the one between side and bottom is relatively small. SCC I and SCC III show slightly larger differences between ITZ porosity at the top and the bottom of aggregates than SCC FA and SCC II (Fig. 9).

The concentration of portlandite in SCC I increases as the aggregates are approached (Fig. 10). The increase at the top, the side and the bottom of the aggregates is almost identical. In contrast, the

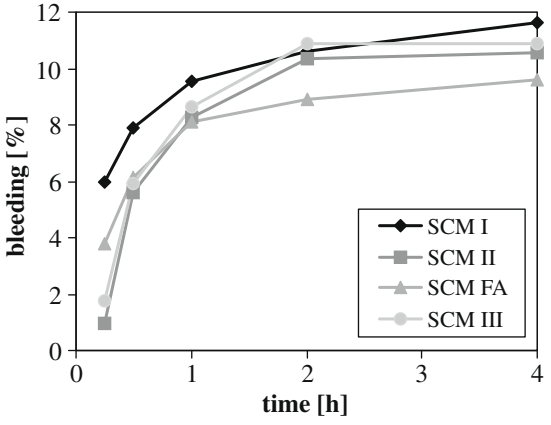

Fig. 4. Cumulative bleeding of SCM in relation to the total amount of mixing water versus time.

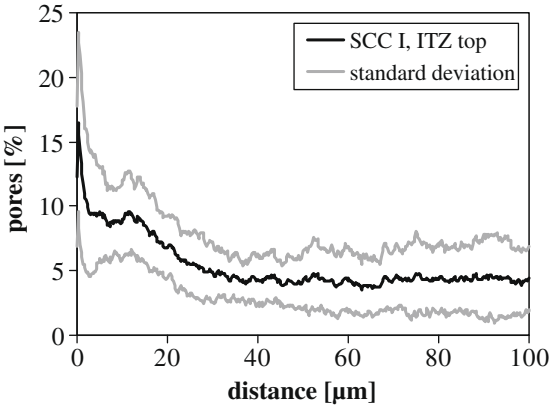

Fig. 6. Volume distribution of pores and its standard deviation in the ITZ at the top of aggregates in SCC I. 30 Images analysed.

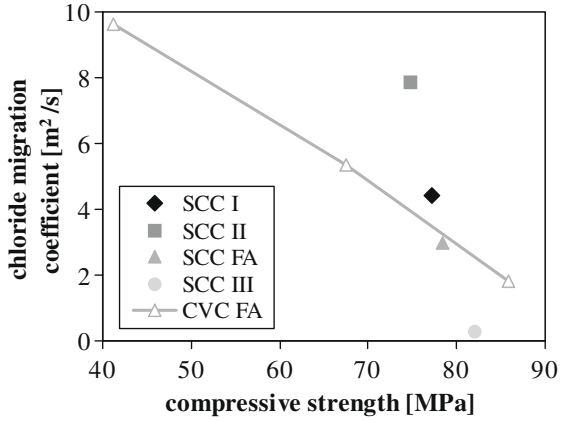

Fig. 5. Chloride migration coefficient versus compressive strength at the age of 64 days.

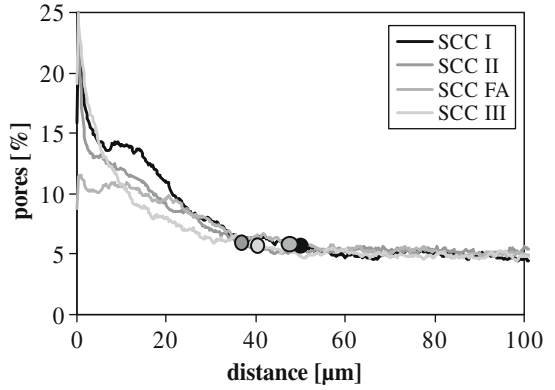

Fig. 7. Volume distribution of pores in the ITZ of the different SCC mixtures. The dots mark the boundary between bulk paste and ITZ. 90 Images analysed per SCC.

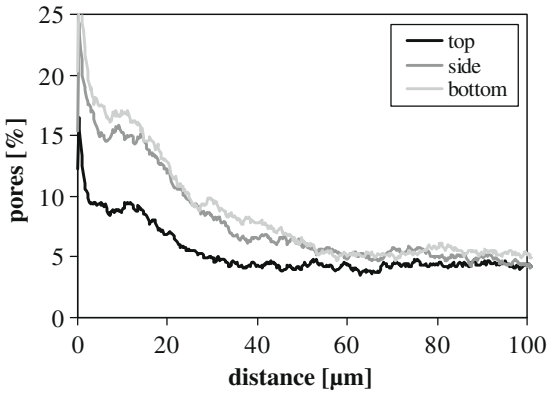

Fig. 8. Volume distribution of pores in the ITZ of SCC I. 90 Images analysed.

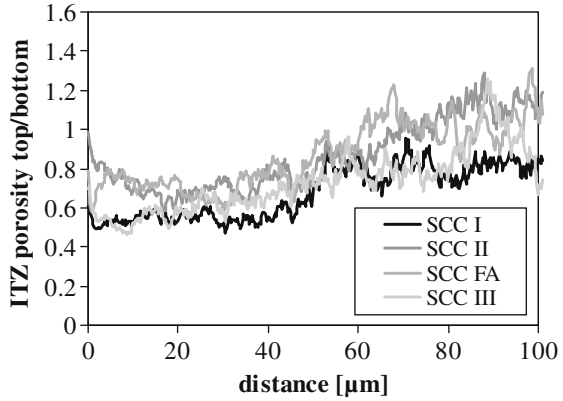

Fig. 9. Ratio between ITZ porosity at the top and the bottom of the aggregates. 90 Images analysed per SCC.

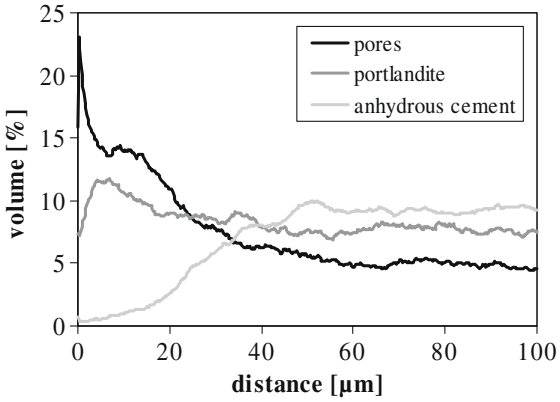

Fig. 10. Volume distribution of pores, portlandite and anhydrous cement in the ITZ of SCC I. 90 Images analysed.

volume of anhydrous cement is decreasing towards the aggregates. The decrease at the top starts closer to the aggregates compared to the side and the bottom. The same applies to anhydrous cement and slag in SCC III (Fig. 11). However, the amount of anhydrous binder in SCC III is larger in the bulk paste and the decrease starts closer to the aggregates compared to SCC I.

4. Discussion

The investigated cements show no differences in bleeding behaviour. Consequently, no relation between the amount of bleeding water and the ITZ porosity at the bottom and the side

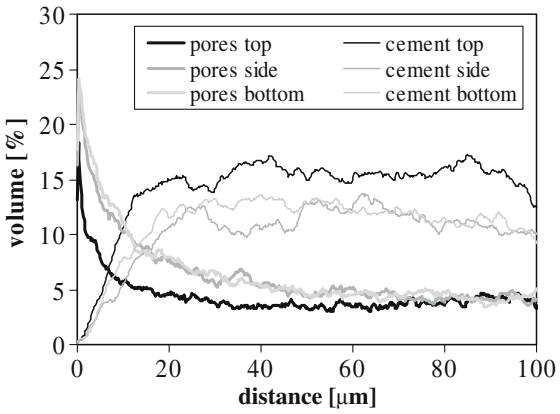

Fig. 11. Volume distribution of pores and anhydrous cement (including slag) in the ITZ of SCC III. 90 Images analysed.

of the aggregates can be observed. Anhydrous cement and slag occur closer to the aggregates at the top compared to the side and the bottom. This indicates sedimentation of cement particles at the top. Accumulation of pore water and sedimentation are the reason for the substantial differences in ITZ porosity between the side/bottom and the top of aggregates.

The decrease of anhydrous binder appearing in a larger distance from the aggregates in SCC I than in SCC III is mainly caused by a combined effect between particle packing and degree of hydration. Firstly, the amount of fine-grained particles is increased close to the aggregate. Secondly, the fine-grained OPC particles close to the aggregates are already fully hydrated in SCC I, while the slow reacting slag particles in SCC III are still anhydrous.

The differences in ITZ thickness of the SCC mixtures are small. However, SCC II and SCC III being produced with finer-grained binders than SCC I and SCC FA have a slightly lower ITZ thickness. This can be interpreted as an effect of grain-size dependent particle packing.

When approaching the aggregates, the plateau that interrupts the porosity increase in SCC I is due to the increased precipitation of portlandite in this relatively porous area. This applies as well for SCC II and SCC FA. SCC III contains the lowest amount of cement clinker leading to the smallest amount of portlandite. Therefore it lacks this plateau. The relatively high concentration of portlandite in the ITZ has been reported by various authors [e.g. 7,20].

The influence of ITZ porosity on permeability is apparent when the same type of binder is used [12]. On the one hand, the differences in ITZ porosity of the four SCC mixtures are small, and total porosity is the same, since the same amount of water has been used for their production. On the other hand, the chloride migration coefficients are significantly different. Grain size distribution and composition of the binders determine the pore characteristics and accordingly, the permeability as well. As an example, the addition of slag to cement increases the volume of small pores together with the chloride binding capacity and likewise lowers the permeability [21–23]. In contrast, the addition of limestone powder to cement can increase porosity and permeability [24–26]. These effects are apparent in the measured chloride migration coefficients. Consequently, in SCC the effect of binder type and the resulting pore characteristics are significantly more important for permeability than the pore volume in the ITZ.

5. Conclusions

In this paper, the porosity in the interfacial transition zone of SCC mixtures produced with four different binders is analysed

and compared with their bleeding behaviour and their chloride resistance.

It is found that the porosity in the ITZ of all four SCC is higher compared to the porosity of the bulk paste, while all SCC mixtures show a similar width of the ITZ. It is also observed that the pores in the ITZ and in the bulk paste are distributed inhomogeneously.

The precipitation of portlandite at the aggregate surface produces a less porous area within the ITZ in the SCC I, SCC II and SCC FA mixtures. Due to a low amount of cement clinker, less portlandite precipitates at the aggregate surface in the SCC III mixture and as a consequence this area of reduced porosity is missing.

ITZ porosity at the top of aggregates is always substantially lower compared to the side and the bottom of the aggregates. This is due to the sedimentation of particles and the accumulation of pore water respectively.

As there is no significant difference in bleeding behaviour of the different cements, no relation between bleeding and ITZ porosity can be retrieved.

The substantial differences in the chloride migration coefficient of the different SCC mixtures show that in these mixtures the binder type and the associated specific pore characteristics of the bulk cement paste have a significantly stronger impact on permeability than the pore volume in the ITZ.

References

[1] Farran J. Contribution mineralogique à l'étude de l'adherence entre les constituants hydrates des ciments et les materiaux enrobes. Rev Mater Construct 1956;490/491:191–209.

[2] Scrivener KL, Crumbie AK, Pratt PL. A study of the interfacial region between cement paste and aggregate in concrete. In: Mindess S, Sha SP, editors. Bonding in cementitious composites. Materials Research Society; 1988. p. 87–95.

[3] Winslow DN, Cohen MD, Bentz DP, Snyder KA, Garboczi EJ. Percolation and pore structure in mortars and concrete. Cem Concr Res 1994;24:25–37.

[4] Garboczi EJ, Bentz DP. Modelling of the microstructure and transport properties of concrete. Construct Build Mater 1996;10:293–300.

[5] Scrivener KL, Nemati KL. The percolation of pore space in the cement paste/aggregate interfacial zone of concrete. Cem Concr Res 1996;26:35–40.

[6] Scrivener KL, Bentur A, Pratt PL. Quantitative characterisation of the transition zone in high strength concrete. Adv Cem Res 1988;1:230–7.

[7] Crumbie AK. Ph.D thesis, University of London; 1994.

[8] Diamond S, Huang J. The interfacial transition zone: reality or myth? In: Katz A, Bentur A, Alexander M, Arliguie G, editors. The interfacial transition zone in cementitious composites. London: E. & F.N. Spoon; 1998. p. 1–37.

[9] De Schutter G, Audenaert K. Durability of self-compacting concrete. RILEM report 38. Bagneux, France: RILEM Publications S.A.R.L.; 2007.

[10] Skarendahl A, Petersson Ö. Self-compacting concrete – state-of-the-art report. RILEM report 23. Cachan Cedex, France; 2001.

[11] Hoffmann C, Leemann A. Homogeneity of structures made with self-compacting concrete and conventional concrete. In: Wallevik O, Nielsson I, editors. Proceedings 3rd int RILEM symposium SCC,. Reykjavik, Iceland; 2003. p. 619–27.

[12] Leemann A, Münch B, Gasser P, Holzer L. Influence of compaction on the interfacial transition zone and the permeability of concrete. Cem Concr Res 2006;36:1425–33.

[13] Okamura H, Ouchi M. Self-compacting concrete: development, present use and future. In: Skarendahl Å, Petersson Ö, editors. Proceedings 1st int RILEM symposium SCC,. Stockholm; 1999. p. 3–14.

[14] Ferraris CF, Obla KH, Hill R. The influence of mineral admixtures on the rheology of cement paste and concrete. Cem Concr Res 2001;31:245–55.

[15] Park CK, Noh MH, Park TH. Rheological properties of cementitious materials containing mineral admixtures. Cem Concr Res 2005;35:842–9.

[16] Vikan H, Justnes H. Rheology of cementitious paste with silica fume or limestone. Cem Concr Res 2007;37:1512–7.

[17] EN 12390-3. Testing hardened concrete – part 3: compressive strength of test specimens; 2002.

[18] Schweizer Ingenieur- und Architektenverein, Betonbau – Ergänzende Festlegungen, Anhang B: Chloridwiderstand. Schweizer Norm 505, No. 262/1; 2003.

[19] Loser R, Lothenbach B, Leemann A, Tuchschmid M. Chloride resistance of concrete and its binding capacity - comparison between experimental results and thermodynamic modeling. Cem Concr Compos 2010;32:34–42.

[20] Scrivener KL, Crumbie AK, Laugesen P. The interfacial transition zone (ITZ) between cement paste and aggregate in concrete. Interf Sci 2004;12:411–21.

[21] Niu Q, Feng N, Yang J, Zheng X. Effect of superfine slag powder on cement properties. Cem Concr Res 2002;32:615–21.

[22] Luo R, Cai Y, Wang C, Huang X. Study of chloride binding and diffusion in GGBS concrete. Cem Concr Res 2003;33:1–7.

[23] Quellet S, Bussière B, Aubertin M, Benzaazoua M. Microstructural evolution of cemented paste backfill: mercury intrusion porosimetry test results. Cem Concr Res 2007;37:1654–65.

[24] Tsivilis S, Chaniotakis E, Batis G, Meletiou C, Kasselouri V, Kakali K, et al. The effect of clinker and limestone quality on the gas permeability, water absorption and pore structure of limestone cement concrete. Cem Concr Compos 1999;21:139–46.

[25] Tsivilis S, Tsantilas J, Kakali G, Chaniotakis E, Sakellariou A. The permeability of Portland limestone cement concrete. Cem Concr Res 2003;33:1465–71.

[26] Matschei T, Lothenbach B, Glasser FP. The role of calcium carbonate in cement hydration. Cem Concr Res 2007;37:551–8.